CHEMISTRY
A EUROPEAN JOURNAL

DOI: 10.1002/chem.200501295

Multiple-Functional Capsule Catalysts: A Tailor-Made Confined Reaction Environment for the Direct Synthesis of Middle Isoparaffins from Syngas

Jingjiang He,[a] Zhenlin Liu,[a] Yoshiharu Yoneyama,[a] Norikazu Nishiyama,[b] and Noritatsu Tsubaki*[a]

Abstract: A capsule catalyst for isoparaffin synthesis based on Fischer–Tropsch reaction was designed by coating a H-ZSM-5 membrane onto the surface of the pre-shaped Co/SiO_2 pellet. Morphological and chemical analysis showed that the capsule catalyst had a core-shell structure. A compact, integral shell of H-ZSM-5 crystallized firmly on the Co/SiO_2 substrate without crack. Syngas passed through the zeolite membrane to reach the Co/SiO_2 catalyst to be converted, and all hydrocarbons formed with straight chain structure must enter the zeolite channels to undergo hydrocracking as well as isomerization in this tailor-made confined reaction environment. A narrow, anti-Anderson–Schultz–Flory law product distribution was observed on these capsule catalysts. Contrary to a mechanical mixture of H-ZSM-5 and Co/SiO_2, C_{10+} hydrocarbons were suppressed completely on this novel capsule catalyst, and the selectivity of middle isoparaffins was considerably improved. The carbon number distribution of the products depended on the thickness of the zeolite membrane, and it was possible to selectively synthesize specified distillates, such as gasoline-range, or heavier hydrocarbons from syngas directly, by simply adjusting the thickness of the zeolite membrane of the capsule catalyst. This kind of capsule catalysts can be extended to various consecutive reaction systems as the shell and core components are independent catalysts for different reactions. At the same time, shape selectivity and space-confined effects can be expected for the reactant, intermediates and product of the sequential reactions.

Keywords: capsules · Fischer–Tropsch synthesis · heterogeneous catalysis · membranes · zeolites

Introduction

The Fischer–Tropsch synthesis (FTS) reaction, described by Fischer and Tropsch in 1923,[1] is a process which yields hydrocarbons from syngas (CO/H_2). The advantages of FTS products over conventional petroleum-derived products are their sulphur-free, aromatic-free, and nitrogen-free properties.[2–7] This makes the FTS products ideal candidate for fuel preparation, as well as starting material to other chemicals. With the technological development of producing syngas from a great variety of sources, such as coal, natural gas, and biomass,[8] the FTS process is becoming more promising.[9] However, all FTS products are normal aliphatic hydrocarbons and their distribution follows the Anderson–Schultz–Flory (ASF) law. It is difficult to selectively obtain hydrocarbons with a narrow, specified carbon number distribution from the FTS reaction,[10,11] unless an additional procedure is employed, such as addition of 1-olefin, or in supercritical phase reaction media.[12–14] Furthermore, FTS products are normal hydrocarbons, which are suitable as diesel fuel only. In order to be used as gasoline, they must further be hydrocracked and isomerized to branched, light hydrocarbons in a separate reaction. Therefore, it is of great industrial interest to design hybrid catalysts for the FTS reaction to directly produce hydrocarbons of certain carbon number distribution and with a branched structure at the same time. Several groups have tried to synthesize isoparaffins by utilizing FTS catalysts made of metal supported on zeolites.[15–17] These catalysts, however, suffered from very low CO conversion for their extremely low reduction degree

[a] Dr. J. He, Dr. Z. Liu, Dr. Y. Yoneyama, Prof. Dr. N. Tsubaki
Department of Applied Chemistry
School of Engineering
University of Toyama
Gofuku 3190, Toyama 930-8555 (Japan)
Fax: (+81) 76-445-6846
E-mail: tsubaki@eng.u-toyama.ac.jp

[b] Dr. N. Nishiyama
Division of Chemical Engineering
Graduate School of Engineering Science
Osaka University
Osaka 560-8531 (Japan)

originated from the strong interaction between the metal and zeolite.

It is well known that zeolites have special pore structures.[18–20] At the same time, zeolites are also good hydrocracking/hydroisomerization catalysts due to its acidic properties.[21] Recently we reported that when a hybrid catalyst of mechanically mixed zeolite and Co/SiO_2 FTS catalyst was used in single or dual step FTS reaction, the formation of short-chain isoparaffins was enhanced while that of long-chain hydrocarbons was suppressed.[22–24] We designed a new catalyst by coating a zeolite membrane directly onto the surface of FTS Co/SiO_2 pellet termed "capsule catalyst".[25] Syngas passed through the zeolite membrane to reach the Co/SiO_2 catalyst and all hydrocarbons subsequently formed must enter the zeolite channels to be hydrocracked and isomerized. The structure of this newly designed catalyst was studied thoroughly with physicochemical characterization methods and its catalytic performances were tested and compared with those of the conventional Co/SiO_2 catalyst and the mechanical mixture catalyst.

Results

Structure of the capsule catalysts: The structural and chemical properties of the capsule catalysts are summarized in Table 1. The surface area of the Co/SiO_2 dropped from 323.0 m^2g^{-1} (SiO_2) to 269.8 m^2g^{-1} because of the impregnation and calcinations procedure, while it slightly increased after the coating of H-ZSM-5 membrane. The weight of the H-ZSM-5 membrane increased with the crystallization time. Accordingly, the surface area increased while the pore volume decreased with the crystallization time. For smaller pellet size, the H-ZSM-5 membrane was coated easier, as indicated in the weight increment of the Co/SiO_2-Z-M and Co/SiO_2-Z-S samples even with only one day of synthesis. The pure H-ZSM-5 had larger specific surface area (432.5 m^2g^{-1}) and smaller pore volume (0.38 cm^3g^{-1}) than SiO_2, and these properties determined the increased surface area and the decreased pore volume of H-ZSM-5 coated catalysts.

The XRD patterns of these samples are shown in Figure 1. Peaks of H-ZSM-5 and Co_3O_4 can be distinguished clearly. The Co_3O_4 particle size was similar for all catalysts, including the precursor Co/SiO_2 catalyst, as listed in Table 1. This indicates that the membrane coating process did not affect the Co cluster size on the SiO_2 surface. The peak intensity of zeolite increased with the crystallization time, which also proved that the zeolite-loading amount increased with the crystallization time. On the patterns of Co/SiO_2-Z-M and Co/SiO_2-Z-S (Figure 1f and g), the ratio of the first two peaks (around 10°) of H-ZSM-5 was different from that of pure H-ZSM-5 (Figure 1h). It seems that the crystallization of H-ZSM-5 on the SiO_2 substrate with smaller pellet size was anisotropic.[26]

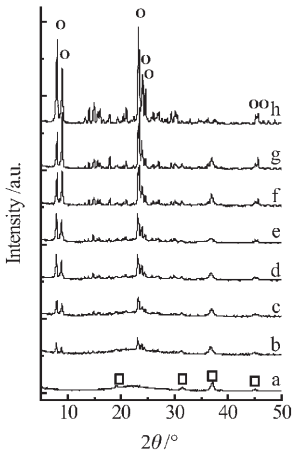

Figure 1. XRD patterns of the samples. a) Co/SiO_2; b) Co/SiO_2-Z-X; c) Co/SiO_2-Z-1; d) Co/SiO_2-Z-2; e) Co/SiO_2-Z-7; f) Co/SiO_2-Z-M; g) Co/SiO_2-Z-S; h) H-ZSM-5; ○: H-ZSM-5, □: Co_3O_4.

The surface acidity of the samples was tested by NH_3-TPD and the total NH_3 uptakes on samples are listed in Table 1. The NH_3 uptake on pure H-ZSM-5 was 281 $\mu mol\,g^{-1}$. The trace amount of ammonia uptake on Co/SiO_2 catalyst suggests that there were few acidic sites. The TPD profiles are shown in Figure 2. Two desorption peaks are clearly observed on pure H-ZSM-5 (Figure 2d); the peak close to 353 K is attributed to the physically adsorbed NH_3, and the other in the 623–643 K range is related to the acidic sites on the zeolite surface.[27–29] The capsule catalysts give two desorption peaks at the similar temperature range and the peak intensity increases with the crystallization time. The capsule catalyst prepared from the small SiO_2 pellet showed the largest ammonia uptake. The amount of adsorbed NH_3 increased linearly with the zeolite loading, as shown in Figure 3, indicating that the properties of the acidic site were the same despite of the changed crystallization time, but the amount of the acidic site increased with the crystallization time.

Table 1. Morphological and chemical properties of the capsule catalysts.

Sample	Surface area [m^2g^{-1}]	Pore volume [cm^3g^{-1}]	Weight increment after zeolite coating [%]	NH_3 uptake [$\mu mol\,g^{-1}$cat.]	Size of Co_3O_4 crystalline [nm]
Co/SiO_2	269.8	1.024	0	9.3	12
Co/SiO_2-Z-1	275.3	0.529	11.5	47.0	11
Co/SiO_2-Z-2	286.1	0.406	17.2	56.8	12
Co/SiO_2-Z-7	310.9	0.282	24.3	76.4	13
Co/SiO_2-Z-M	358.6	0.202	29.1	102.4	13
Co/SiO_2-Z-S	372.6	0.178	29.6	105.2	13

Figure 4 shows the SEM images of the external surfaces of the Co/SiO_2 FTS catalyst and the capsule catalyst Co/SiO_2-Z-2. The H-ZSM-5 crystallites can be clearly observed on the capsule catalyst. The surface elemental analysis by EDX in Figure 5 confirmed the integrity of the zeolite membrane on the

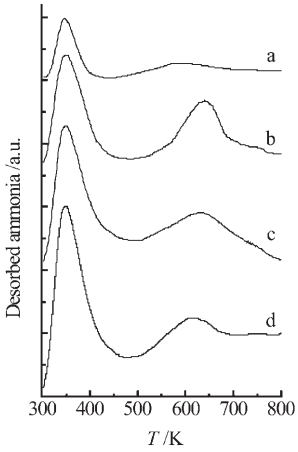

Figure 2. NH_3/TPD profiles of the H-ZSM-5 zeolite and the capsule catalysts. a) Co/SiO_2-Z-1; b) Co/SiO_2-Z-2; c) Co/SiO_2-Z-7; d) H-ZSM-5.

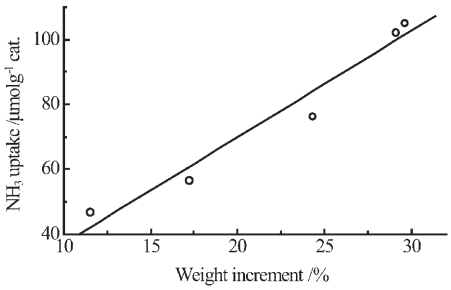

Figure 3. Relationship between the NH_3 uptake and the weight of the zeolite membrane.

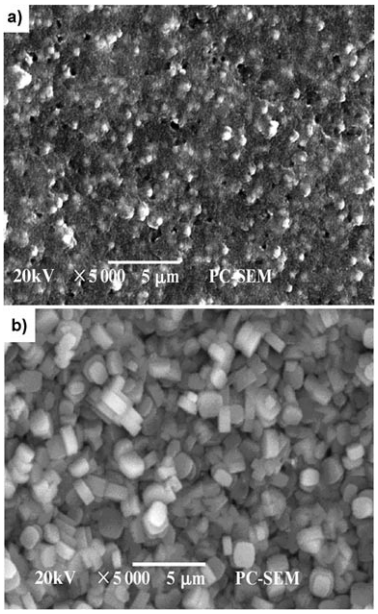

Figure 4. SEM images of the external surface of the Co/SiO_2 pellet and the capsule catalyst pellet, and the EDS analysis result. a) Co/SiO_2; b) Co/SiO_2-Z-2.

Co/SiO_2 pellet. On the Co/SiO_2 surface, $Co_{K\alpha}$ and $Co_{L\alpha}$ peaks were clearly detected; while on Co/SiO_2-Z-2, there

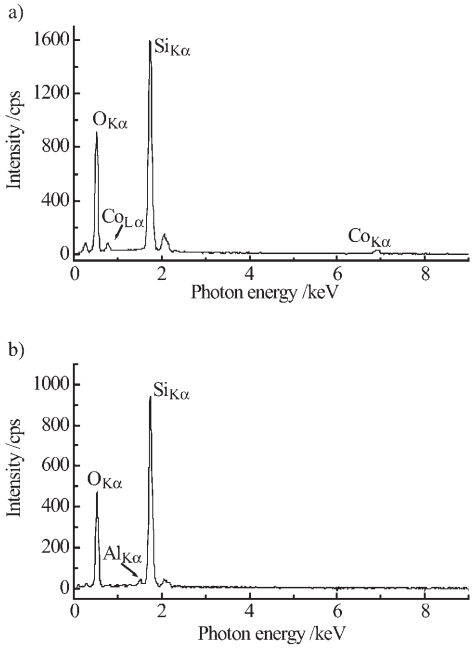

Figure 5. Elemental composition of the external surface of the Co/SiO_2 pellet and the capsule catalyst pellet from EDX analysis. a) Co/SiO_2; molar ratio: Al 0.00%, Si 90.66%, Co 9.14%; b) Co/SiO_2-Z-2; molar ratio: Al 2.21%, Si 97.79%, Co 0.00%.

was no signal of Co, suggesting that there was no pinhole or crack in the zeolite membrane. The SiO_2/Al_2O_3 ratio from the EDX analysis was 88.

Figure 6 shows the SEM images and the radial elemental analysis of the section of the capsule catalyst pellets. A compact H-ZSM-5 shell can be clearly observed crystallizing on the surface of Co/SiO_2 substrate. At the interface between the Co/SiO_2 substrate and the H-ZSM-5 membrane, the radial distribution of Si dropped suddenly while that of Al increased slightly, which indicates a change from the SiO_2 to the H-ZSM-5 phase. However, the Al composition was not zero inside the Co/SiO_2 substrate, which confirms that the H-ZSM-5 entered the pores of the Co/SiO_2. The same phenomena are found on all three samples with varied crystallization time. The membrane thickness was measured as 2.3, 7.6, and 23.1 μm for crystallization of 1, 2, and 7 days, respectively. From the Si signal intensity distribution inside the zeolite shell as shown in Figure 6a–c, Co/SiO_2-Z-7 exhibited a flatter line than the other two catalysts, indicating that longer synthesis time in zeolite preparation was beneficial to obtain a membrane with uniform structure. From the SEM images and the radial elemental analysis, we can also draw the conclusion that the thickness of H-ZSM-5 shell can be controlled by the crystallization time.

The experimental results above confirmed that a compact H-ZSM-5 membrane without cracks was directly synthesized on the surface of all Co/SiO_2 pellets by hydrothermal method.

FTS reaction of capsule catalysts: The catalytic performance of the pure Co/SiO_2, the mechanically mixed Co/SiO_2-Z-X,

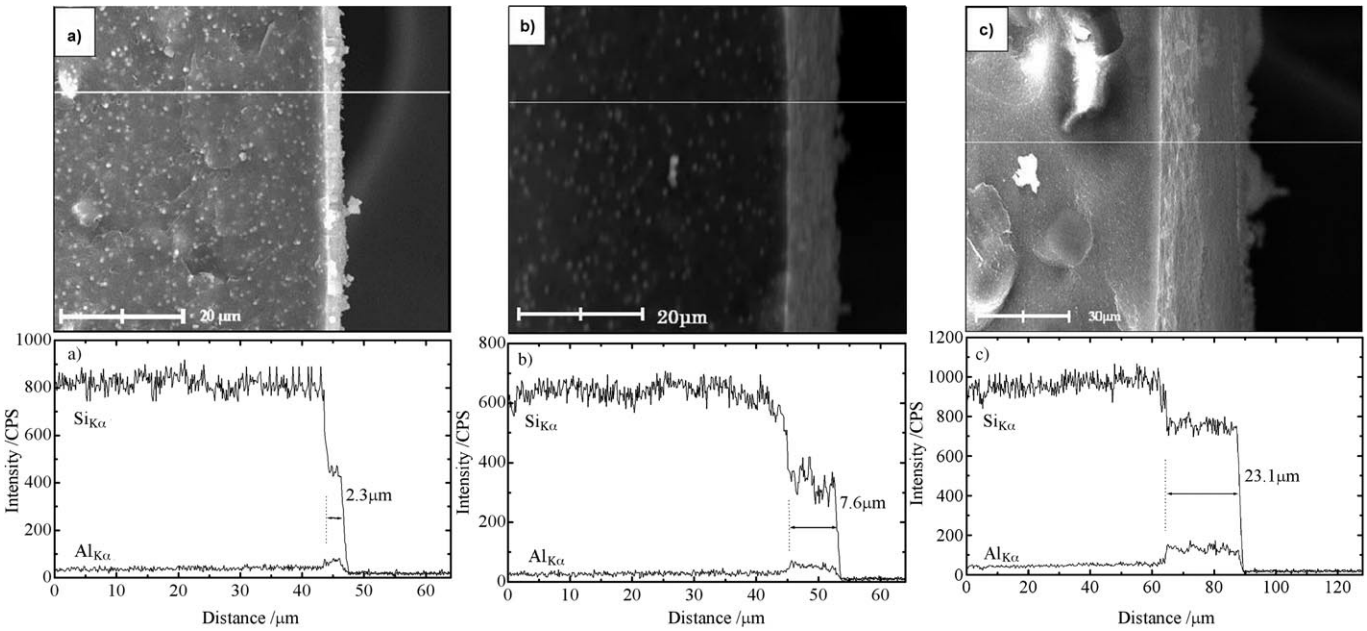

Figure 6. Cross-sectional SEM images and the radial elemental distribution of Al and Si by the EDX analysis. a) Co/SiO_2-Z-1; b) Co/SiO_2-Z-2; c) Co/SiO_2-Z-7.

and the capsule catalysts was tested and the results are presented in Table 2. The product distributions on these catalysts are shown in Figures 7 and 8. The CO conversion, CH_4 and CO_2 selectivity of the mechanically mixed Co/SiO_2-Z-X were almost the same as those of the pure Co/SiO_2, although significant amounts of isoparaffins and olefins were formed. From Figure 7, it can be seen that the Co/SiO_2-Z-X gives a more narrow product distribution. The waxy product from the conventional FTS catalyst, which remains on the surface of the catalysts, was subjected to the secondary reactions of isomerization and hydrocracking on the acidic sites of the zeolite, and subsequently converted to lighter hydrocarbons containing isoparaffins. The sequential isomerization and hydrocracking reactions on the zeolite reduced the selectivity of the long-chain paraffins and remarkably enhanced the selectivity of the light isoparaffins. However, there were still heavy paraffins formed on the mechanically mixed Co/SiO_2-Z-X, distributed until C_{20}.

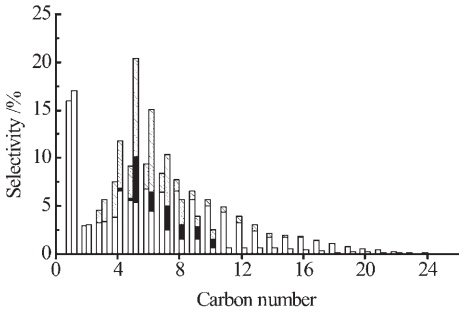

Figure 7. Product distributions on the pure Co/SiO_2 and the mechanically mixed Co/SiO_2-Z-X catalysts at 533 K. In each carbon number group, left: pure Co/SiO_2, right: Co/SiO_2-Z-X; □: *n*-paraffin, ■: isoparaffin, \\\ olefin.

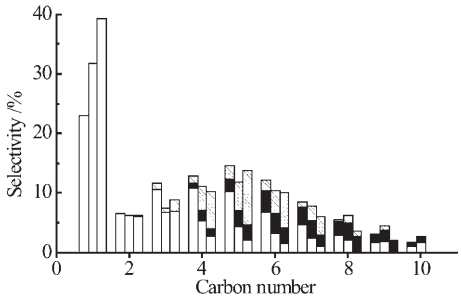

Figure 8. Product distributions on the capsule catalysts with varied crystallization time. In every data group, left: 1 d, middle: 2 d, and right: 7 d; □: *n*-paraffin, ■: isoparaffin, \\\ olefin.

All three capsule catalysts with a hydrothermal time of 1, 2, and 7 days showed a similar CO conversion, which was about 10% lower than that of Co/SiO_2 or Co/SiO_2-Z-X. The slightly lower activity is ascribed to the coverage of a part of the Co active sites by the zeolite coating. The zeolite membrane might restrict the adsorption of CO and H_2 onto the active Co sites to some extent. However, the activity did not decrease with the increased thickness of the zeolite coating, which indicates that the rate-controlling step was not the diffusion of the syngas through the zeolite membrane, but the FTS reaction itself on the Co sites, at least under the present reaction conditions, especially the reaction temperature. Nevertheless, it is difficult to exclude the possibility that small zeolite pore might lower the diffusion rate of the syngas reaching the core FTS catalyst. The methane selectivity was higher on the capsule catalysts and it increased with the zeolite membrane thickness. Because H_2 diffuses more quickly than CO, especially inside small pores or channels,

Table 2. Effect of the zeolite crystallization time, and the Co/SiO_2 pellet size on the catalytic performance of the capsule catalysts.[a]

Sample	CO conversion [%]	CH_4 selectivity [%]	CO_2 selectivity [%]	C_{iso}/C_n[b]	$C^{=}/C_n$[c]
Co/SiO_2	98.4	15.7	10.6	0	0.28
Co/SiO_2-Z-X	93.6	16.9	8.0	0.49	1.09
Co/SiO_2-Z-1	83.6	22.7	10.0	0.37	0.14
Co/SiO_2-Z-2	85.5	31.3	10.2	0.73	0.51
Co/SiO_2-Z-7	86.1	37.4	7.0	1.88	1.35
Co/SiO_2-Z-M	91.5	24.3	10.4	1.21	0.85
Co/SiO_2-Z-S	89.1	22.4	6.9	0.74	0.63

[a] Reaction conditions: 533 K, 1.0 MPa, $W_{Co/SiO_2}/F = 10\ g\,h\,mol^{-1}$, $H_2/CO = 2/1$. [b] C_{iso}/C_n is the ratio of isoparaffin to *n*-paraffin of C_{4+}. [c] $C^{=}/C_n$ is the ratio of olefin to *n*-paraffin of C_{2+}.

the lower diffusion efficiency of CO led to a high H_2/CO ratio in the interior part of the catalyst pellet, which might increase methane selectivity.[30] The selectivity of isoparaffins as well as olefins increased with zeolite thickness. The isoparaffins selectivity on the Co/SiO_2-Z-7 was remarkably higher than that on the Co/SiO_2-Z-X, although the zeolite content in both catalysts was similar: 24% zeolite in the Co/SiO_2-Z-7, and 20% zeolite in the Co/SiO_2-Z-X.

In order to test the effect of reaction temperature, FTS was carried out on the Co/SiO_2-Z-1 and Co/SiO_2-Z-2 samples under 513, 523, 533, 543, and 553 K, respectively. The results are shown in Table 3 and the product distributions

Table 3. Effect of the reaction temperature T_r on the catalytic performance of the capsule catalysts.[a]

Sample	T_r [K]	CO conversion [%]	CH_4 selectivity [%]	CO_2 selectivity [%]	C_{iso}/C_n	$C^{=}/C_n$
Co/SiO_2-Z-1	513	70.6	15.9	3.9	0.32	0.23
	523	73.1	17.5	4.0	0.37	0.26
	533	83.6	22.7	10.0	0.37	0.14
	543	94.7	34.2	21.8	0.44	0.08
	553	97.1	38.2	24.4	0.44	0.04
Co/SiO_2-Z-2	513	71.1	25.3	5.3	0.30	0.37
	523	84.5	28.1	9.5	0.56	0.50
	533	85.5	31.3	10.2	0.73	0.51
	543	98.8	44.3	28.1	0.78	0.14
	553	99.8	51.8	30.9	0.77	0.15

[a] Reaction conditions: 1.0 MPa, $W_{Co/SiO_2}/F = 10\ g\,h\,mol^{-1}$, H_2/CO 2:1.

are shown in Figures 9 and 10. The CO conversion, CH_4 and CO_2 selectivity on the capsule catalyst increased with temperature. After desorption from the Co sites on the SiO_2 surface, the hydrocarbons underwent isomerization and hydrocracking reaction at the acidic sites of H-ZSM-5. At elevated temperature, the isomerization reaction was accelerated, consequently the isoparaffins increased. It is obvious that the elevated temperature favoring light hydrocarbons is due to the accelerated hydrocracking on zeolite and the decreased chain growth probability of the FTS itself. From Table 3, it is also interesting that the olefin selectivity is decreasing with higher reaction temperatures.

Figure 11 shows the product distributions of the two catalysts prepared from middle and small-size Co/SiO_2 pellet. Compared with the results of the Co/SiO_2-Z-1 catalyst, which was also crystallized for one day, the membrane was easier to coat onto the smaller-size pellet and resulted in a higher isoparaffin/*n*-paraffin ratio as shown in Table 2. This indicates that the pellet size of the core catalyst had a strong effect on the capsule catalyst property. The modification of either or both the membrane catalyst and the core catalyst, or optimizing the reaction condition might further enhance the catalytic activity and selectivity of the capsule catalysts.

Discussion

Analysis of the designed structure of the tailor-made capsule catalyst: In the capsule catalyst, the zeolite mainly consisting of silica has enough affinity to the silica surface of the Co/SiO_2 substrate. It can be assumed that the Si-O-H groups from the Co/SiO_2 surface and the zeolite combined to form Si-O-Si bonds, anchoring the zeo-

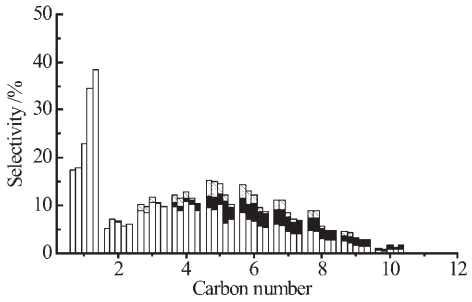

Figure 9. Product distributions on Co/SiO_2-Z-1 catalyst at varied reaction temperature. From left to right in every data group, the reaction temperature increased from 513 to 553 K, at 10 K intervals; □: *n*-paraffin, ■: isoparaffin, \\\ olefin.

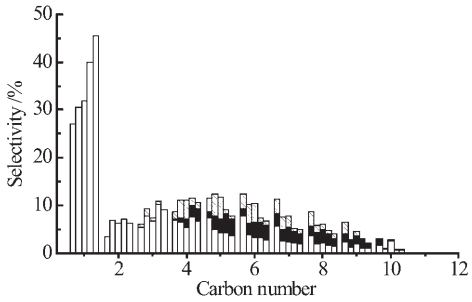

Figure 10. Product distributions on Co/SiO_2-Z-2 catalyst at varied reaction temperature. From left to right in every data group, the reaction temperature increased from 513 to 553 K, at 10 K intervals; □: *n*-paraffin, ■: isoparaffin, \\\ olefin.

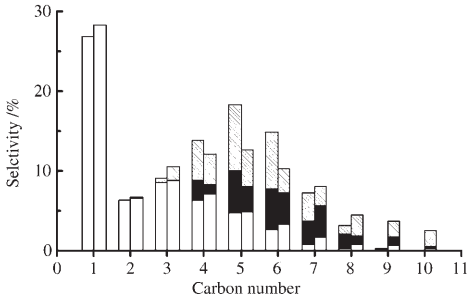

Figure 11. Product distributions on the capsule catalysts of 1 day crystallization with different pellet size of the Co/SiO_2 precursor. In every data group, left: 0.38–0.50 mm, and right: 0.18–0.25 mm; □: *n*-paraffin, ■: isoparaffin, \\\ olefin.

lite membrane enveloping the Co/SiO_2 core. Of course the Al-O-Si bonds were also possible to increase the strength of combination between the zeolite shell and the Co/SiO_2 core. As in Figure 6, small amounts of Al entered the Co/SiO_2 core, indicating that some part of the zeolite membrane formed inside the pores of Co/SiO_2 catalyst and strengthened the combination. Luckily, Al_2O_3 is also widely used as cobalt FTS catalyst support and has no negative effect on FTS catalyst even if coexists with silica.

To check the stability of the core-shell structure of the capsule catalyst, we used ultrasonic experiments (0.5 kW, 6 h, 5 g catalyst dispersed in 30 mL water) to test the stability of the obtained capsule catalyst and found that the structure of the capsule catalyst was still maintained and separation of the membrane from the core was not observed. Considering the thin and delicate structure of the zeolite membrane, we only used a fixed bed reactor. The catalyst is probably not suitable for slurry phase or fluidized bed reactor.

Figure 4b shows Co/SiO_2-Z-2 where the catalyst was hydrothermally treated for two days. As in Figure 6b, the thickness of this Co/SiO_2-Z-2 was 7.6 μm. Thickness of 2.3 μm was for Co/SiO_2-Z-1 where the catalyst was hydrothermally treated for one day. It can not be expected that the whole zeolite membrane formed as a single crystal. The membrane here was built up by zeolite crystals with the size of 1–5 μm. As depicted in Figure 6, longer hydrothermal synthesis times favored the formation of ZSM-5 membranes with a more uniform structure although the pellet size of the core Co/SiO_2 was also important. As shown in Tables 1 and 2 as well as Figure 11 the time of membrane coating descreased with smaller Co/SiO_2 pellets.

If the zeolite membrane is very thick, the diffusion rate of syngas will be lowered as the zeolite pore is not large. On the other hand, if the zeolite membrane is very thin, the amount of acidic sites is so limited that the rate of hydrocracking and isomerization will be lowered. The membrane thickness may be optimized, and depends on the rate balance between the FTS and the hydrocracking/isomerization, reaction temperature, zeolite type, and so on.

Effect of the space-confined reaction environment on FTS: The capsule catalysts gave completely different product distribution compared with normal FTS catalysts. Not only is the product distribution deviant from the ASF law, but also the heavy paraffins of C_{11+} were completely suppressed. The product distribution of the mechanical mixture did not follow the ASF law as well, but there were still C_{11}–C_{20} products. This difference was caused by the unique core-shell structure of the capsule catalyst. For the mechanical mixture of Co/SiO_2-Z-X, there was no spatial restriction between the two reactions of FTS and hydrocracking/isomerization. The hydrocarbons desorbed from the FTS site might leave the catalyst directly without undergoing cracking on the zeolite sites. With the capsule catalyst structure, all hydrocarbons with straight-chain molecular structure could enter the zeolite channels and be cracked at the acidic sites of zeolite. Since the hydrocarbon diffusion rate in the zeolite membrane depends on the chain length, the longer the chain length, the longer the hydrocarbons will stay inside the zeolite and the higher the chance that they will be cracked as illustrated in Figure 12.

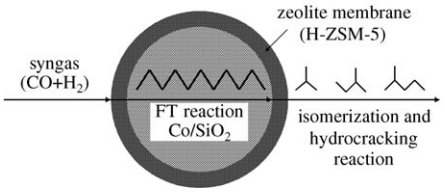

Figure 12. Schematic image of the reaction procedure on the capsule catalyst.

Furthermore, compared with conventional membrane reactors, the capsule catalyst has larger membrane area per unit reactor volume. This property was also the reason for the high selectivity of the isoparaffin on the capsule catalyst, besides its core-shell structure. Of course, with this catalyst preparation the difficulties of preparing large-area membrane without aperture or cracking can be avoided.[31]

Even if the isoparaffin obtained has a larger steric hindrance than its linear analogue, all cracked products have smaller molecular weights and diffuse through the zeolite channels quickly to the outer surface. Furthermore, the concentration of linear FTS paraffins at the entrance of the zeolite channel at the inner surface of membrane was significantly higher than that at the channel entrance of the outer surface, this concentration gradient was a driving force to push the lighter cracked products to the outer surface, even if the cracked products were branched by isomerization and/or hydrocracking.

Olefins also formed to some extent in the FTS reaction on the capsule catalysts. It can be assumed that if the olefin is hydrogenated, the isoparaffin selectivity can be enhanced furthermore. In Table 3, the olefin selectivity was lowered at higher reaction temperatures as the olefin formed can be readsorbed onto cobalt sites to be hydrogenated, especially

at higher temperatures. Consequently, higher C_{iso}/C_n ratio and lower $C^{=}/C_n$ ratio was obtained at higher temperatures; this proves that a large amount of branched olefins was included in the olefin. Higher temperatures will increase the CH_4 selectivity in FTS, while lowering the selectivity of total heavier hydrocarbons. Alternatively it is possible to introduce Pd or Pt species to the ZSM-5 membrane to selectively hydrogenate olefin, including branched olefins at lower temperature. Meanwhile, the introduction of Pd or Pt might stabilize the zeolite activity and decrease the coke formation effectively through the spillover effect, which will be discussed below.

Stability and reaction characteristics of the capsule catalyst: The conventional gas-phase Fischer–Tropsch synthesis (FTS) requires an induction period to reach steady-state conditions because of its polymerization character. The waxy hydrocarbons accumulate on the FTS catalyst surface and deactivate the catalyst. While on the capsule catalyst, the zeolite membrane can decompose the waxy products in situ, the steady state is reached faster. Also, the temperature control in the conventional gas-phase FTS is another problem which disturbs the steady state as the FTS is an exothermal reaction. Luckily, on the capsule catalyst the exothermal FTS and the endothermic hydrocracking of linear FTS hydrocarbons are integrated as a consecutive reactions mode. Hydrocracking reactions can absorb in situ FTS reaction heat, which leads to a quick arrival of the steady state. The 100 h reaction test is shown in Figure 13 where the CO conversion, *iso*-to-

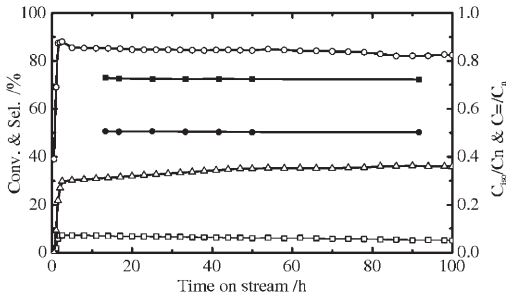

Figure 13. Reaction performance of 100 h continuous FTS using Co/SiO_2-Z-7. Standard reaction conditions; temperature: 533 K; ○ CO conversion, ■: C_{iso}/C_n, ●: $C^{=}/C_n$, △: CH_4 selectivity, CO_2 selectivity.

normal ratio, olefin-to-paraffin ratio, the methane and CO_2 selectivity were stable during the entire experimental period. Another possibility of the zeolite membrane stability may come from the metallic cobalt at the core FTS catalyst, as the supported cobalt particles exist very closely to the zeolite membrane with intimate contacts in the capsule catalyst. It is deduced that cobalt here might also activate gaseous hydrogen to stabilize the catalytic activity of the zeolite, acting similarly to Pd in Pd/SiO_2 + zeolite mixed catalyst system.[32]

Concerning the increased methane selectivity, as mentioned above, the diffusion rate of H_2 is faster than that of CO; also, a higher H_2/CO ratio might appear after the syngas passed through the zeolite channel, leading to higher methane selectivity in the core Co/SiO_2 FTS catalyst inside capsule catalyst. Furthermore, the 1-olefin from hydrocracking of FTS normal paraffin seems to be cracked easily to release methane at acidic sites.[33]

Even after longer reaction times, the capsule catalyst did not change its color and the carbon balance remained between 98–102%. The surface chemical composition of the used capsule catalyst was analyzed by EDX, and it was found that the carbon signal was very low and negligible.

The thermal gravimetry analysis was conducted for the fresh and used capsule catalysts and the results are shown in Figure 14. The weight loss below 400 K should be from the water removal. The weight loss above 500 K is due to the coke combustion. Curve C is for the used Co/SiO_2 catalyst without zeolite where waxy hydrocarbons accumulated heavily. Curve B is very flat, indicating the zeolite decomposed the waxy products efficiently. From the slight difference between curve A of the fresh capsule catalyst and curve B of the used capsule catalyst, it is clear that the carbon deposition on the used Co/SiO_2-Z-7 capsule catalyst is negligible and practically did not influence the stability of the capsule catalyst even after working for 100 h.

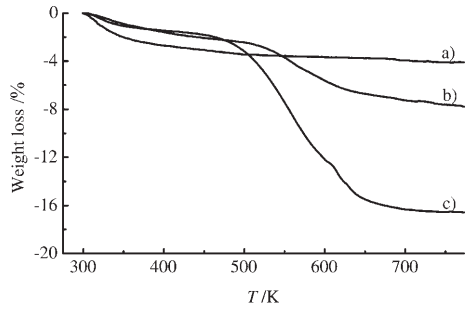

Figure 14. Weight loss of thermal gravity curves of different catalyst. a) fresh Co/SiO_2-Z-7; b) used Co/SiO_2-Z-7 after 100 h reaction; c) used Co/SiO_2 catalyst after 6 h.

Conclusion

By the improved hydrothermal synthesis method, the H-ZSM-5 membrane was successfully coated onto the Co/SiO_2 catalyst pellet to form a new kind of capsule catalyst. With the increase of the crystallization time, the zeolite loading increased, and so did the membrane thickness. Although the total CO conversion on these capsule catalysts was slightly lower, they exhibited a better selectivity for light hydrocarbon synthesis, especially for isoparaffin synthesis from syngas than the mechanical mixture of the catalyst. The formation of long chain hydrocarbons of C_{11+} was suppressed completely by the zeolite membrane in this confined reaction environment. Smaller pellet size of the core Co/SiO_2 catalyst significantly improved the catalytic properties of this novel capsule catalyst. The combination of the two se-

quential reactions by the capsule catalyst, a new reaction environment with spatial selectivity and shape selectivity may open a wide industrial application for the heterogeneous catalysis process.

Experimental Section

Catalyst preparation: The conventional Co/SiO_2 FTS catalyst was prepared by incipient wetness impregnation method. Silica (Cariat Q-10, Fuji Silysia Chemical Ltd., specific surface area 323.0 $m^2 g^{-1}$, pore volume 1.03 $cm^3 g^{-1}$, mean pore diameter 10 nm), with three different pellet sizes of 0.85–1.7 mm (large), 0.38–0.50 mm (middle), and 0.18–0.25 mm (small), was used as support. The aqueous solution of $Co(NO_3)_2 \cdot 6H_2O$ with appropriate concentration was used to yield 10 wt% Co loading in all samples. The catalyst precursors were dried in air at 393 K for 12 h, and then calcined in air at 673 K for 2 h.

The H-ZSM-5 membrane was synthesized in the solution of deionized water and ethanol, with TPAOH (tetrapropylammonium hydroxide) as template, $Al(NO_3)_3 \cdot 9H_2O$ and TEOS (tetraethyl orthosilicate) as Al and Si sources, respectively, with a SiO_2/Al_2O_3 ratio of 80:1. The molar ratio of the reactant was: $TPAOH/Al(NO_3)_3/TEOS/EtOH/H_2O$ 0.25:0.025:1:4:60. Firstly, TEOS, TPAOH, ethanol and water were added into a 100 mL Teflon tank. The $Al(NO_3)_3 \cdot 9H_2O$ was carefully added to the mixture solution, which was stirred at 333 K for 2 h until a lucid sol was formed. After the Co/SiO_2 pellet was added into the sol, the tank was capped and set in the hydrothermal synthesis equipment (DRM-420DA, Hiro Company, Japan). The crystallization of the zeolite was carried out at 453 K and a rotation speed of 10 rpm for 1, 2, and 7 d, respectively, to test the effect of crystallization time on the membrane structure. Finally, the coated catalyst was separated from the synthesis solution and dried at 393 K for 12 h, followed by calcination at 773 K for 5 h. The catalysts were designated as Co/SiO_2-Z-(*n*), where last number refers to the crystallization time in days with Co/SiO_2 substrate with large pellet size. X refers to the mechanical mixture of H-ZSM-5 and Co/SiO_2, with a weight ratio of (Co/SiO_2):H-ZSM-5 = 4:1. M and S mean that the capsule catalysts were prepared from Co/SiO_2 with middle and small pellet size for 1 d. The pure H-ZSM-5 was also synthesized by the same method without the addition of the Co/SiO_2 substrate for 1 d. All the chemicals were supplied by Wako Pure Chemicals Ltd., if not indicated specifically.

Catalyst characterization: The specific surface area and the pore volume of the samples were determined by N_2 adsorption at 77 K using an automatic gas adsorption system (Quantachrome, Autosorb-1, Yuasa Co.). Prior to measurements, the samples were degassed at 573 K and 3.0 Pa.

The morphology of the samples was investigated with a scanning electron microscopy (SEM) equipped with an energy-diffusive X-ray spectroscopy (EDX) attachment (JEOL JSM-6360LV), which could simultaneously provide the surface elemental composition information. The catalyst was pre-coated with Pt before introduced into the vacuum chamber.

The XRD patterns were obtained on a RINT 2400 powder diffractometer (Rigaku Co.) in a step mode employing $Cu_{K\alpha}$ radiation ($\lambda = 0.154$ nm). The X-ray tube was operated at 40 kV and 40 mA. The mean crystalline size of Co_3O_4 was calculated based upon the Scherrer equation.

The temperature programmed desorption (TPD) of NH_3 was carried out in a flow system. The samples were first purged in He at 473 K for 1 h, and then cooled down to 423 K to be saturated with NH_3 for 30 min. Helium gas was switched to again remove the residual gaseous NH_3 until no signal in the effluent could be detected by the down stream gas chromatograph (GC, TCD). The desorption profiles were obtained under the following conditions: flow rate 50 mL min^{-1} He, and ramping rate 5 K min^{-1} from 300 K to 800 K.

Thermal gravimetry experiment was conducted to investigate the possible coke formation on the catalyst. It was implemented in air flow on a Shimadzu machine (DTG-60). Temperature was increased from 298 to 773 K at a rate of 5 K min^{-1}.

Fischer–Tropsch synthesis (FTS) reaction test: The FTS reactions were conducted in a continuous flow type fixed-bed reactor in the temperature range of 513 to 553 K under a pressure of 1.0 MPa. The catalyst with 0.5 g Co/SiO_2 was loaded in the center of the stainless steel reactor (i.d. 8 mm) and reduced in situ at 673 K for 10 h in H_2 flow, followed by cooling down to 353 K in N_2 before exposure to syngas. When the desired reaction temperature was reached, pressurized syngas (CO/H_2, molar ratio $^1/_2$, $W_{Co/SiO_2}/F = 10$ g h mol^{-1}) was introduced and the reaction was carried on continuously for 6–100 h. An ice trap with the solvent and inner standard was set between the reactor and the back pressure regulator to capture the heavy hydrocarbons in the effluent. A trap with concentrated sulfuric acid was set after the back pressure regulator to absorb the olefins, since the separation of olefins and isoparaffins by the gas chromatograph column was not so satisfying. The concentration of light hydrocarbons (C_1–C_{10}) was analyzed with an online gas chromatograph (GC-FID, Shimadzu, GC-14B) equipped with a capillary column (J&W Scientific GS-Alumina, i.d. 0.53 mm, length = 30 m) for separating the iso- and *n*-paraffins. To check the possible formation of isoparaffins higher than C_{10}, a high-temperature distillation-type gas chromatograph (HP-6890) was used for each reaction with zeolite-containing catalyst, but no hydrocarbons higher than C_{10} was detected. When testing the activity of the catalysts without zeolite coating, because of the presence of heavy components in the effluent, a silicone SE-30 column was used instead of the capillary column to avoid jamming of the capillary column. The condensate hydrocarbons (C_{4+}) in the ice trap were collected after the reaction and also analyzed with the GC-FID by injection. The two results were summed up to calculate the yields of the iso- and *n*-paraffins. The yields of the olefins were obtained from the difference of the GC peaks before and after the olefins were absorbed in the H_2SO_4 trap. The concentration of CO, CO_2, and CH_4 in the effluent from the reactor was monitored with an online GC-TCD (Shimadzu, GC-8A) equipped with an active charcoal column. To prevent the middle hydrocarbons (C_5–C_9) from entering the GC-TCD, an ice trap filled with water was set before the six-way valve leading to the GC-TCD. For zeolite-coated catalysts, *n*-heptane was used as the inner standard, and *n*-octane as the solvent in the trap. For catalysts without zeolite coating, *n*-heptadecane was used as the inner standard, and *n*-tridecane as the solvent.

[1] G. Henrici-Olive, S. Olive, *The Chemistry of the Catalyzed Hydrogenation of Carbon Monoxide*, Springer, Tokyo, **1984**, p. 144.
[2] E. Iglesia, S. L. Soled, R. A. Fiato, *J. Catal.* **1992**, *137*, 212–224.
[3] B. G. Johnson, C. H. Bartholomew, D. W. Goodman, *J. Catal.* **1991**, *128*, 231–247.
[4] D. Schanke, S. Vada, E. A. Blekkan, A. M. Hilman, A. Hoff, A. Holmen, *J. Catal.* **1995**, *156*, 85–95.
[5] G. P. Van Der Laan, A. Beenackers, *Catal. Rev. Sci. Eng.* **1999**, *41*, 255–318.
[6] E. Iglesia, *Appl. Catal. A* **1997**, *161*, 59–78.
[7] S. Li, S. Krishnamoorthy, A. Li, G. D. Meitzner, E. Iglesia, *J. Catal.* **2002**, *206*, 202–217.
[8] H. L. Chum, R. P. Overend, *Fuel Process. Technol.* **2001**, *71*, 187–195.
[9] J. E. Wegrzyn, D. Mahajan, M. Gurevich, *Catal. Today* **1999**, *50*, 97–108.
[10] R. B. Anderson, *The Fischer-Tropsch Synthesis*, Academic Press, New York, **1984**.
[11] J. Patzlaff, Y. Liu, C. Graffmann, J. Gaube, *Appl. Catal. A* **1999**, *186*, 109–119.
[12] N. Tsubaki, K. Fujimoto, *Fuel Process. Technol.* **2000**, *62*, 173–186.
[13] N. Tsubaki, K. Yoshii, K. Fujimoto, *J. Catal.* **2002**, *207*, 371–375.
[14] K. Fujimoto, L. Fan, K. Yoshii, *Top. Catal.* **1995**, *2*, 259–266.
[15] Y. W. Chen, H. T. Tang, J. G. Goodwin, Jr., *J. Catal.* **1983**, *83*, 415–427.
[16] H. H. Nijs, P. A. Jacobs, *J. Catal.* **1980**, *66*, 401–411.
[17] P. A. Jacobs in *Catalysis by Zeolites* (Eds.: B. Imelik, C. Naccache, J. C. Vedrine), Elsevier, Amsterdam, **1980**, p. 293.
[18] R. M. de Vos, H. Verweij, *Science* **1998**, *279*, 1710–1711.

[19] N. Nishiyama, M. Miyamoto, Y. Egashira, K. Ueyama, *Chem. Commun.* **2001**, *18*, 1746–1747.
[20] Z. Lai, G. Bonlla, I. Diaz, J. G. Nery, K. Sujaoti, M. A. Amat, E. Kokkoli, O Terasaki, R. W. Thompson, M. D. Tsapatsis, G. Vlachos, *Science* **2003**, *300*, 456–460.
[21] A. Feller, A. Guzman, I. Zuazo, J. A. Lercher, *J. Catal.* **2004**, *224*, 80–93.
[22] X. Li, K. Asami, M. Luo, K. Michiki, N. Tsubaki, K. Fujimoto, *Catal. Today* **2003**, *84*, 59–65.
[23] J. He, B. Xu, Y. Yoneyama, N. Nishiyama, N. Tsubaki, *Chem. Lett.* **2005**, 34, 148–149.
[24] T. Zhao, Y. Yoneyama, N. Tsubaki, *Ind. Eng. Chem. Res.* **2005**, *44*, 755–769.
[25] J. He, Y. Yoneyama, B. Xu, N. Nishiyama, N. Tsubaki, *Langmuir* **2005**, *21*, 1699–1702.
[26] Further details on the crystal structure investigations may be obtained from the Fachinformationszentrum Karlsruhe, 76344 Eggenstein-Leopoldshafen (Germany), (fax: (+49) 7247-808-666; e-mail: crysdata@fiz-karlsruhe.de), on quoting the depository numbers CSD-68734 (H-ZSM-5) and CSD-9362 (Co_3O_4).
[27] H. Ichibashi, M. Kitamura, *Catal. Today* **2002**, *73*, 23–28.
[28] R. Q. Long, R. T. Yang, *J. Catal.* **2001**, *198*, 20–28.
[29] F. Lonyi, J. Valyon, *Microporous Mesoporous Mater.* **2001**, *47*, 293–301.
[30] R. J. Madon, E. Iglesia, *J. Catal.* **1994**, *149*, 428–437.
[31] N. Nishiyama, K. Ichioka, D. H. Park, Y. Egashira, K. Ueyama, L. Gora, W. Zhu, F. Kapteijn, J. A. Moulijn, *Ind. Eng. Chem. Res.* **2004**, *43*, 1211–1215.
[32] K. Fujimoto, I. Nakamura, *Stud. Surf. Sci. Catal.* **1997**, *112*, 29–38.
[33] Y. Zhang, M. Koike, N. Tsubaki, *Catal. Lett.* **2005**, *99*, 193–198.

Received: October 19, 2005
Revised: March 24, 2006
Published online: July 19, 2006

